SENSORLESS BROKEN BAR DETECTION IN INDUCTION MACHINES

Hakan ÇALIŞ[1] **Abdülkadir ÇAKIR[1]** **Müslüm ARKAN[2]**
[1] *e-posta: hcalis@tef.sdu.edu.tr* [1] *e-posta: cakir@tef.sdu.edu.tr* [2] *e-posta: markan@inonu.edu.tr*
[1] *Department of Electronics –Computer Education The Faculty of Technical Education*
Suleyman Demirel University, 32260, Çünür- Isparta
[2] *Department of Electrical- Electronics Engineering The Faculty of Engineering,*
Inonu University –Malatya

Key Words: Broken bar, Fault detection, Induction machine

ABSTRACT

This study describes broken bar detection in induction motors before actual breakdown occurs. It is based on fluctuations of stator current Zero-Crossing Times (ZCT). Instead of sampling motor current with an high resolution A/D converter, zero crossing instants are recorded as waveforms cross zero. Fluctuations in the intervals between successive zero-crossings of the three phase current waveforms are analysed using Fast Fourier Transforms (FFT). Rotor bar faults are identifiable from amplitude changes of $2sf_s$ spectral component where *s* is the motor slip.

I. INTRODUCTION

There are two kinds of induction rotating motors, the squirrel-cage motor and the wounded rotor motor. Since the squirrel-cage induction motor is low-priced, robust and rugged, simple and easy to maintain, it has become the most commonly used electrical rotating machine in industry. It is becoming increasingly important to use condition monitoring techniques to give early warning of imminent failure. Detection of broken rotor bar at particularly an early stage, is rather difficult than stator faults. On the one hand, rotor bar faults are usually associated with the high temperatures attained in the rotor, and the high mechanical loading on the end rings of the cage, particularly during starting time. On the other hand, faults may occur during manufacture process, either through defective casting in the case of die cast rotors, or through poor jointing in the case of brazed or welded end rings. Such a defect in rotor will result in a high resistance which will overheat at that area, and the high temperature will impair the strength of the cage. Cracking or small holes may then occur in the rotor bar. Rotor bar faults are more likely to take place at the cage end rings where the rotor bars are not fully supported by the laminated rotor core.

It is known that the early indications of induction motor rotor bar faults are pulsations in the speed, motor current and stray leakage flux of the machine. A continual attempt to develop new approach for cost-effective, sensitive, reliable and on-line rotor bar failure prediction is always highly encouraged by industry.

Rotor asymmetry can be detected by monitoring the fluctuations in rotor speed [1][9]. However, it is difficult to determine the degree of asymmetry. In addition, an extra sensor (e.g. tachometer) is needed for the monitoring. The disadvantage of this method is that the sensitivity of the measurement depends largely on the inertia of the load, and the amplitude of the speed fluctuations will be much smaller when a high-inertia load is applied to the machine.

Vibration analysis, thermal analysis and current spectrum analysis have been applied to monitor rotor bar faults [1]. Most recent efforts seem to be focusing on current spectrum analysis as the current signal is easily accessible for all induction motors. Practice and theory has demonstrated [2][3] that when a induction motor is supplied by a balanced mains supply of frequency f_s and running at a slip of *s*, there will be a stator frequency component $(1-2s)f_s$ which is induced due to rotor slight unbalance caused by some small hole in the rotor bar. The magnitude of this induced e.m.f. is generally very small compared to the component of the mains, and therefore it is very difficult to detect. It is only possible to detect on full-load, i.e., running with maximum slip *s*. Also, when the load changes during the sampling period the $(1-2s)f_s$ component may smear out. Hsu [6] proposed to use air-gap torque to monitor defects such as cracked rotor bars and shorted stator coils. Elkasabgy et al [8] used an external search coil mounted on the motor frame to analyse the induced voltage waveform.
Some of these techniques will have limited usage, since they either need sophisticated installation with expensive sensors or complicated mathematical modelling and high computational power. In industry however, low cost and

high sensitivity of a motor diagnostic system is highly demanded.

In this study, **Zero-Crossing Times** (*ZCT*) method, invented firstly by Wang in Sussex University, England, to detect broken rotor bars in an induction machine is used [10]. The method is utilised to extract the new characteristic rotor failure component. The *ZCT* method avoids the use of traditional stator current spectrum for rotor defects detection so that the annoying proximate relation between mains frequency component f_s and failure component $(1-2s) f_s$ is no longer a problem. The details of the *ZCT* method for rotor fault detection will be described in following sections. It is shown that the *ZCT* method is both sensitive and low cost. Again, the principle of *ZCT* method can be applied in the variable speed drives or soft starters by software modification only. In addition, an inexpensive and independent stand-alone circuitry can be employed.

.

II. OBTAINING THE ZCT SIGNAL

The *ZCT* signal consists of a series of data values, obtained at each zero crossing time of the 3-phase current. The values of data are defined as the time difference between two adjacent zero-crossing times $(T_n - T_{n-1})$ minus the time interval for *60* degrees $T60$ of the mains supply as shown in figure 1 [10, 11].

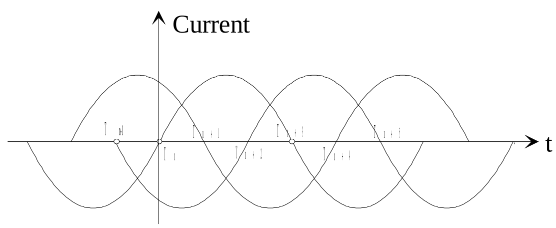

$ZCT_{n+1} = T_{n+1} - T_n - T60$

$T_{n+3} - T_n = T180$

Figure 1 Description of *ZCT* signal

In ideal conditions (perfectly balanced supply and completely symmetrical stator windings) the value of ZCT signal is zero. In practice, it is almost impossible to assume an ideal supply and a complete symmetrical induction motor, which inevitably results in corresponding fluctuations in the 3-phase current zero-crossing times [10,11]. In fact, we have found that the *ZCT* signal carries rich information that reflects both induction motor internal conditions and external influence such as supply unbalance.

III. SIMULATION OF BROKEN BAR FAULTS USING MATLAB/SIMULINK MODEL

In this study, 3Hp, 4 pole squirrel cage induction motor is used for simulations. Block diagram of an induction motor's Simulink model is shown as in figure 2. Rotor bar fault is simulated by externally adding three star connected rotor resistors. The each value of rotor phase resistance, between 0,10Ω and 0,16Ω. is changed in 0,02Ω steps. In addition, zero crossing detection circuit, power spectrum estimation of ZCT and motor current signals are included with displaying and storing in a data file blocks.

In this model, for the each value of rotor resistance amplitude changes in spectrum of stator current and ZCT signals are determined. The simulation results for unloaded motor are shown as in Table 1. Loaded conditions such as 7.5 Nm 15 Nm (half load) and full load (30Nm) are displayed in Table 2, Table 3 and Table 4 sequentially. For unloaded motor, broken bar detection from amplitude changes, in stator current (at f_s ± s f_s components) and ZCT spectrum (at 2s f_s) can not give good results. (see Table 1)

For full load condition whereas amplitude changes (at f_s ± s f_s) in motor current spectrum are very small, magnitude changes of 2s f_s component in ZCT spectrum are more evident even for small rotor bar fault condition (in a 0,02Ω increment). With development of fault, this increment reaches to value of $8.765.10^{-6}$. As shown in figure 3a-b increments on f_s ± s f_s components seem distinct due to scaling vertical axis in dB units. In practice, the amplitude of these sidebands are too small to detect compare to large amplitude of supply frequency (see figure 3a-b). On the other hand, the spectral changes at 2sf in ZCT spectrums in case of rotor bar fault is around –50dB. This variation is still in detectable level for various load conditions. (See figure 4a-b)

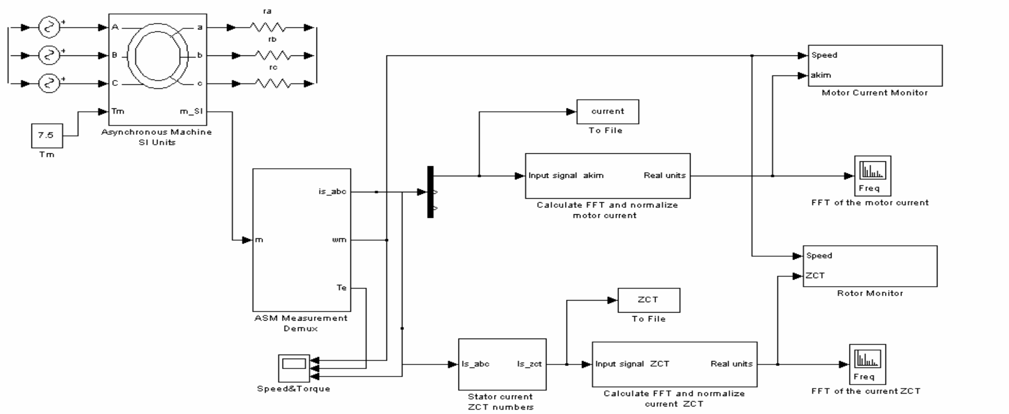

Figure 2 Simulink model of sensorless broken bar detection for induction motor

Table 1 Simulation results for unloaded induction motor

Fault indicator components	**Rotor resistance changes (Ω)**			
CURRENT	**0,1**	**0,12**	**0,14**	**0,16**
2sf	0,0008538	0,0008779	0,0009023	0,0009269
f	9,824	9,824	9,824	9,824
(1-s)f	9,824	9,824	9,824	9,824
(1+s)f	9,824	9,824	9,824	9,824
ZCT	**0,1**	**0,12**	**0,14**	**0,16**
2sf	$1,077.10^{-16}$	$7,462.10^{-17}$	$7,002.10^{-17}$	$7,070.10^{-17}$
2f	$6,752.10^{-15}$	$5,903.10^{-15}$	$4,394.10^{-15}$	$3,150.10^{-15}$
(1-s)2f	$6,752.10^{-15}$	$3,688.10^{-15}$	$3,967.10^{-15}$	$3,150.10^{-15}$
(1+s)2f	$6,570.10^{-15}$	$3,688.10^{-15}$	$3,527.10^{-15}$	$2,969.10^{-15}$

Table 2 Simulation results for loaded induction motor (7,5 Nm)

Fault indicator components	**Rotor resistance changes (Ω)**			
CURRENT	**0,1**	**0,12**	**0,14**	**0,16**
2sf	0,001579	0,001581	0,001709	0,001711
f	10,48	10,48	10,48	10,48
(1-s)f	10,48	10,48	10,48	10,48
(1+s)f	5,214	5,214	5,214	5,214
ZCT	**0,1**	**0,12**	**0,14**	**0,16**
2sf	$6,642.10^{-14}$	$1,529.10^{-7}$	$3,096.10^{-7}$	$4,695.10^{-7}$
2f	$2,8.10^{-13}$	$2,992.10^{-13}$	$3,178.10^{-13}$	$3,411.10^{-13}$
(1-s)2f	$2,8.10^{-13}$	$2,992.10^{-13}$	$3,178.10^{-13}$	$3,411.10^{-13}$
(1+s)2f	$2,8.10^{-13}$	$2,992.10^{-13}$	$3,178.10^{-13}$	$3,411.10^{-13}$

Table 3 Simulation results for half loaded induction motor (15 Nm)

Fault indicator components	**Rotor resistance changes (Ω)**			
CURRENT	**0,1**	**0,12**	**0,14**	**0,16**
2sf	0,002771	0,002769	0,002765	0,002761
f	12,36	12,36	12,36	12,36
(1-s)f	0,02098	0,02037	0,02039	0,02041
(1+s)f	0,02235	0,02208	0,02211	0,02215
ZCT	**0,1**	**0,12**	**0,14**	**0,16**
2sf	$2,776.10^{-13}$	$0,4008.10^{-6}$	$1,234.10^{-6}$	$2,105.10^{-6}$
2f	$1,357.10^{-12}$	$1,04.10^{-12}$	$1,01.10^{-12}$	$0,2376.10^{-12}$
(1-s)2f	$1,457.10^{-12}$	$1,434.10^{-12}$	$0,9476.10^{-13}$	$0,1729.10^{-12}$
(1+s)2f	$4,516.10^{-13}$	$0,919.10^{-12}$	$0,9883.10^{-13}$	$1,493.10^{-12}$

Table 4 Simulation results for fully loaded induction motor (30 Nm)

Fault indicator components	Rotor resistance changes (Ω)			
CURRENT	**0,1**	**0,12**	**0,14**	**0,16**
2sf	0,005611	0,005796	0,005983	0,006257
f	18,32	18,32	18,32	18,32
(1-s)f	0,01724	0,01571	0,01567	0,01563
(1+s)f	0,02117	0,01974	0,01969	0,01964
ZCT	**0,1**	**0,12**	**0,14**	**0,16**
2sf	9,91.10^{-13}	2,716.10^{-6}	5,661.10^{-6}	8,765.10^{-6}
2f	1,136.10^{-12}	1,02.10^{-12}	1,272.10^{-12}	2,292.10^{-12}
(1-s)2f	3,02.10^{-12}	3,11.10^{-12}	3,401.10^{-12}	2,817.10^{-12}
(1+s)2f	2,351.10^{-12}	2,504.10^{-12}	2,701.10^{-12}	3,124.10^{-12}

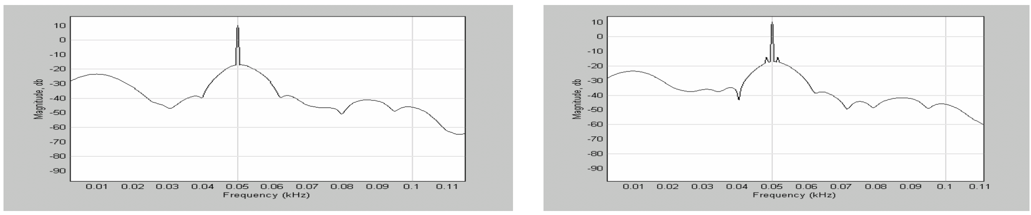

(a) (b)

Figure 3 Motor current spectrums

a-) For ideal rotor (0,1Ω) b-) For faulty rotor bar (0,06Ω increment in rotor resistance)

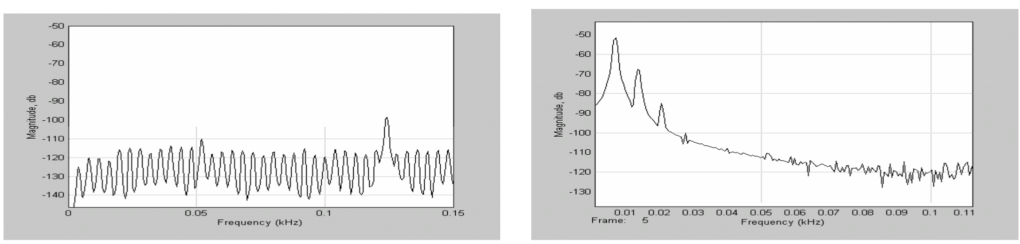

(a) (b)

Figure 4 ZCT Spectrums a) For ideal rotor (0,1Ω) b-) For faulty rotor bar (0,06Ω increment in rotor resistance)

The effect of supply voltage unbalance on rotor bar fault detection characteristic frequency component (2s f_s) is examined as shown in Table 5. Separation of these two faults, simultaneously occurred is realized the monitoring of 2 f_s component in ZCT spectrum. Fault indicator component 2s f_s can still be used when motor supplied from unbalanced voltage source. $2f_s$ Frequency component appears only when supply is unbalance. Motor current and ZCT spectrums are shown in Figure 5-6 respectively for mixed faults.

Table 5 Simulation results for fully loaded motor supplied by unbalanced voltage source (216V 1.8 % decrement in voltage level) for various broken bar level

Fault indicator components	Rotor resistance changes (Ω)			
CURRENT	**0,1**	**0,12**	**0,14**	**0,16**
2sf	0,00171	0,001709	0,001708	0,001707
f	9,576	9,576	9,576	9,576
(1-s)f	9,576	9,576	9,576	9,576
(1+s)f	4,764	4,764	4,764	4,764
ZCT	**0,1**	**0,12**	**0,14**	**0,16**
2sf	5,129.10^{-12}	1,602.10^{-7}	3,238.10^{-7}	5,105.10^{-7}
2f	0,0004231	0,0004227	0,0004222	0,0004219
(1-s)2f	0,0004231	0,0004227	0,0004222	0,0004219
(1+s)2f	0,0004231	0,0004227	0,0004222	0,0004219

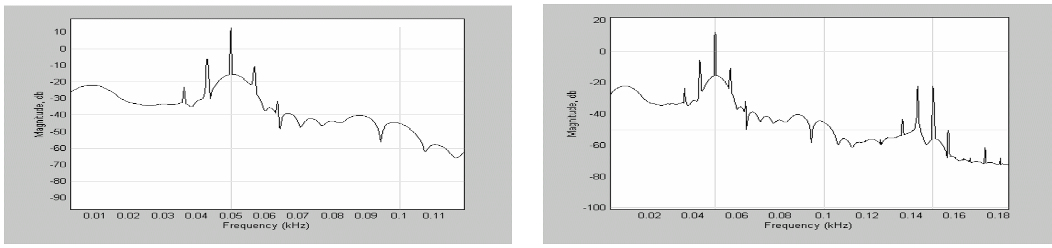

(a) (b)

Figure 5 Motor current spectrums of faulty rotor bar (0,06Ω increment in rotor resistance)
a) Balanced supply b) Unbalanced supply

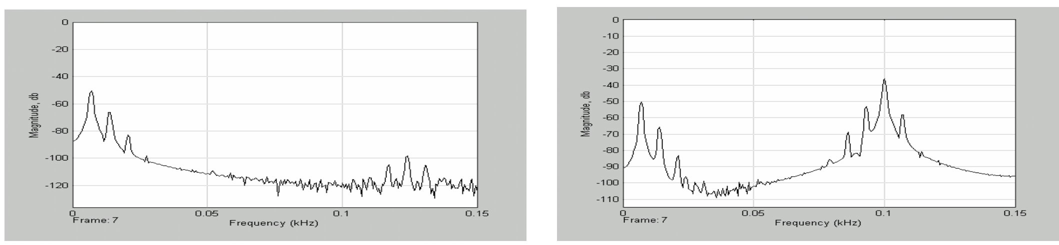

(a) (b)

Figure 6 ZCT spectrums of faulty rotor bar (0,06 Ω increment in rotor resistance)
a) Balanced supply b) Unbalanced supply

IV. CONCLUSIONS

Broken bar detection in three phase induction motors is implemented with ZCT method instead of using traditional supply current monitoring in frequency domain. Motor model is simulated in Matlab/Simulink environment and broken bar faults are simulated by adding extra rotor resistance. The amplitude changes in 2s f_s characteristic frequency component of ZCT signal is monitored clearly. The main advantage of ZCT method is not requiring fast sampling rate and high resolution A/D converter. It may be necessary to include additional signals such as motor vibration or temperature to extend reliability of fault detection system for critical machines. In the next stage of work is going to be implementation of the ZCT method as online detection using Goertzel's algorithm.

REFERENCES

1. **Vas, P**., Parameter Estimation, Condition Monitoring, and Diagnosis of Electrical Machines, *Claredon Press, OXFORD, UK*, 1993.
2. **Ho, S. L.** (1991). Condition Monitoring of Induction Motors, *Fifth International Conference on Electrical Machines and Drives, London, U.K.* pp. 56-60.
3. **Kliman, G. B., Stein, J. and Endicott, R. D.**,(1988), Non-invasive Detection of Broken Rotor Bars in Operating Induction Motors , *IEEE Transactions on Industry Application*, Vol. 3, No. 4, pp. 873-879.
4. Ho, S. L., Chan, W. L. and Leung H. W. (1993). **Application of Statistical Signal Processing for Condition Monitoring of Rotor Faults in Induction Motor** , *Sixth International Conference on Electrical Machines and Drives, Oxford, U.K.* pp. 97-102.
5. Jiang, J. G., Zhang, Z. P., Su, P. S. and Wang, X. H.,(1992) **Time Frequency Spectrum (TFS) of Line Current During Starting Process --- A Tool for Diagnosing Failure of Induction Motor** *International Conference on Electrical Machine. Vol 3, UMIST, Manchester, U.K.* pp. 1261-1265.
6. Hsu, J. S. (1994). **Monitoring of Defects in Induction Motors Through Air-gap Torque Observation**, *IEEE IAS Annual Meeting.*
7. Watson, J. F., Elder, S. (1992). Transient Analysis of the Line Current as a Fault Detection Technique for 3-phase Induction Motors, *International Conference on Electrical Machine. Vol 3, UMIST, Manchester, U.K.* pp. 1241-1245.
8. **Elkasabgy, N. M., Eastham, A. R. and Dawson, G. E.** (1992) Detection of Broken Bars in the Cage Rotor on an Induction Machine , *IEEE Transactions on Industry Application, Vol. 28, No.1*, pp. 165-171.
9. **Tavner P. J., Penman J**. (1987) **Condition Monitoring of Electrical Machines**, *Research Studies Press Ltd., U.K.*

10. **Wang, Y.,** “The *ZCT* Method of Induction Motor Failure Prediction and Speed Monitoring”, Phd Thesis, University of Sussex, England, 1997
11. **Gürdal, O., Cesur O.,** 'A New Sensorless Speed Detection Method By Fluctuation of Zero Crossing Time Signals in Induction Motors', Journal of Polytechnic vol:2 no:1, pp. 43-51, Ankara 1999.
12. **Boyle, C. and et al. :** “Online Current Monitoring to Detect Misalignment and Dynamic Eccentricity in Three Phase Induction Motor Drives”, Proc. 29th Power Engineering Conf., Vol 1, pp 5-8,1994, Ireland.
13. **Bruel & Kjaer :** “Vibration Diagnostics for Industrial Electric Motor Drives”, Application Note.
14. **Dorrell, DG. and et al. :** “Analysis of Air-gap Flux, Current, and Vibration Signals as a Function of the Combination of Static and Dynamic Air-gap Eccentricity in 3-Phase Induction Motors”, IEEE Tran. On Industry Applications Vol 33, No 2, January/February 1997.
15. **Farag, S.F. , et al :** “An Integrated On-Line Motor Protection System” , IEEE IAS Annual Meeting, October 1994.
16. **Kliman, GB, et al .:** “ Methods of Motor Current Signature Analysis “ , Electrical Machines & Power Systems , Vol 20 , (5) , pp463-74 , 1992.
17. **Kliman, GB, et al .:** “ Induction Motor Fault Detection via Passive Current Monitoring” , Electrical Machines & Power Systems , Vol 20 , (5) , pp463-74 , 1992.
18. **Leith, D. and et al ,** “ Real Time Expert System for Identifying Rotor Faults and Mechanical Influences in Induction Motor Phase Current”, IEE 5th ICEM, pp46-50, September 1991.
19. **Penman J, and Tavner P.J.,:** Condition Monitoring of Electrical Machines, Wiley & Sons, New York,1987.
20. **Rao, B.K.N.:** Handbook of condition monitoring, Elsevier Science Ltd, 1996
21. **Schoen, R.R., et al :** “An Unsupervised On-Line System for Induction motor Fault Detection Using Stator Current Monitoring”, IEEE IAS Annual Meeting, October 1994
22. **Vas, P.,** Parameter Estimation, Condition Monitoring, and Diagnosis of Electrical Machines, New York, Oxford University , 1993.
23. **Yang, SJ.** Low Noise Electrical Motor, Clarendon Press, UK, 1981.
24. **Çalış, H.**, **Unsworth, P., :**' Fault Diagnosis in Three Phase Induction Machines by Motor Current Signal Analysis', The 1999 IEEE International Symposium on Diagnostic for Electrical Machines, Power Electronics and Drives', University of Oviedo, Spain, September 1999.
25. **Çalış, H., Çakır, A.:** ’State of Art of Fault Diagnosis Technologies’, IMS2001, International Intelligent Manufacturing Systems, Sakarya University, Sakarya, August 2001.